EURASIP Journal on Wireless Communications and Networking 2005:2, 260–269

Analysis of a Combined Antenna Arrays and Reverse-Link Synchronous DS-CDMA System over Multipath Rician Fading Channels

Yong-Seok Kim

Communication Systems Lab, School of Electrical and Electronics Engineering, Yonsei University, 134 Sinchon-Dong, Seodaemun-Gu, Seoul 120-749, Korea
Email: dragon@yonsei.ac.kr

System Development Team, Telecommunication Systems Division, Telecommunication Network, Samsung Electronics, 416 Moetan-3Dong, Yeongtong-Gu, Suwon-City, Gyeonggi-do 442-600, Korea

Keum-Chan Whang

Communication Systems Lab, School of Electrical and Electronics Engineering, Yonsei University, 134 Sinchon-Dong, Seodaemun-Gu, Seoul 120-749, Korea
Email: kcwhang@yonsei.ac.kr

Received 19 May 2004; Revised 6 December 2004; Recommended for Publication by Arumugam Nallanathan

We present the BER analysis of antenna array (AA) receiver in reverse-link asynchronous multipath Rician channels and analyze the performance of an improved AA system which applies a reverse-link synchronous transmission technique (RLSTT) in order to effectively make a better estimation of covariance matrices at a beamformer-RAKE receiver. In this work, we provide a comprehensive analysis of user capacity which reflects several important factors such as the ratio of the specular component power to the Rayleigh fading power, the shape of multipath intensity profile, and the number of antennas. Theoretical analysis demonstrates that for the case of a strong specular path's power or for a high decay factor, the employment of RLSTT along with AA has the potential of improving the achievable capacity by an order of magnitude.

Keywords and phrases: antenna arrays, reverse-link synchronous DS-CDMA, multipath Rician fading channel.

1. INTRODUCTION

CDMA systems have been considered as attractive multiple-access schemes in wireless communication. But these schemes have capacity limitation caused by cochannel interference (CCI) which includes both multiple access interference (MAI) between the multiusers, and intersymbol interference (ISI) arising from the existence of different transmission paths. A promising approach to increase the system capacity through combating the effects of the CCI is the use of spatial processing with an AA at base station (BS), which is also used as a means to harness diversity from the spatial domain [1, 2, 3]. Generally, the AA system consists of spatially distributed antennas and a beamformer which generates a weight vector to combine the array output. Several algorithms have been proposed in the spatial signal processing to design the weights in the beamformer. The application of AA to CDMA has received some attention [4, 5, 6]. For example, a new space-time processing framework for the beamforming with AA in DS-CDMA has been proposed in [4], where a code-filtering approach was used in each receiving antenna in order to estimate the optimum weights in the beamformer.

For a terrestrial mobile system, RLSTT has been proposed to reduce inter-channel interference over a reverse link [7, 8] with the additional benefit of having a lower multiuser detection, or interference cancelation complexity, than asynchronous systems [9]. Reverse-link synchronous DS-CDMA is therefore considered an attractive technology for future mobile communication systems [10, 11, 12] or mobile broadband wireless access. Synchronous transmission in the reverse link can be achieved by adaptively controlling the transmission time in each mobile station (MS). In a similar way to the closed-loop power control technique, the BS computes the time difference between the reference time generated in the BS and the arrival time of the dominant

signal transmitted from each MS, and then transmits timing control bits, which order MSs to "advance" or "delay" their transmission times. The considered DS-CDMA system uses orthogonal reverse-link spreading sequences and the timing control algorithm that allows the mainpaths to be synchronized. This can be readily achieved by state-of-the-art synchronization techniques [9].

However, previous studies [8, 13] have assumed the presence of Rayleigh fading and have neglected the performance benefit of having a specular component in Rician fading channel, which is often characterized in microcellular environments [14, 15]. Even if [16] presents the analysis of the scenario of a direct line-of-sight (LOS) path, it has not considered the use of spatial processing at cell site (CS). Therefore this paper presents the BER analysis of AA receiver in reverse-link asynchronous multipath Rician channels, and analyzes the performance of an improved AA, in which RLSTT is incorporated to effectively make better an estimation of covariance matrices at a beamformer-RAKE receiver through the analysis of the scenario of a direct LOS path, which results in Rician multipath fading. While RLSTT is effective in the first finger at the RAKE receiver in order to reject MAI, the beamformer estimates the desired user's complex weights, enhancing its signal and reducing CCI from the other directions. In this work, we attempted to provide a comprehensive analysis of user capacity which reflects several important factors such as the ratios of the specular component power to the Rayleigh fading power, the shape of multipath intensity profile (MIP), and the number of antennas.

The paper is organized as follows. In Section 2, system and channel models are described. Section 3 contains the main theoretical results quantifying the probability of bit errors for asynchronous and synchronous transmission scenarios. Section 4 shows numerical results mainly focusing on the system bit error rate (BER) performance. Finally, a concluding remark is given in Section 5.

2. SYSTEM AND CHANNEL MODEL

2.1. Transmitter

We consider a single-cell scenario, and both asynchronous and synchronous DS-CDMA reverse link where the CS has the M-element AA, where M is the number of elements in antenna array. The received signals are assumed to undergo multipath Rician fading channels. Assuming K active users ($k = 1, 2, \ldots, K$), the equivalent signal transmitted by user k is presented as

$$s^{(k)}(t) = \sqrt{2p_k}\, b^{(k)}(t) v^{(k)}(t) \cos\left[\omega_c t + \phi^{(k)}\right], \tag{1}$$

where $b^{(k)}(t)$ is the user k's data waveform, and $v^{(k)}(t)$ is a random signature sequence for the user k. It is noted that a random signature sequence is composed of two sequences in the reverse-link synchronous transmission case, that is, $v^{(k)}(t) = a(t) \cdot g^{(k)}(t)$. $a(t) = \sum_{j=-\infty}^{\infty} a_j P_{T_c}(t - jT_c)$ is a pseudonoise (PN) randomization sequence which is common to all users in a cell to maintain the CDMA orthogonality and $g^{(k)}(t) = \sum_{j=-\infty}^{\infty} g_j^{(k)} P_{T_g}(t - jT_g)$ is an orthogonal channelization sequence [7], where we have $P_\tau(t) = 1$ for $0 \le t \le \tau$ and $P_\tau(t) = 0$ otherwise. On the other hand, we assume that there is one constituent sequence of random signature sequence in the asynchronous case, that is, $v^{(k)}(t) = a^{(k)}(t)$, where $a^{(k)}(t) = \sum_{j=-\infty}^{\infty} a_j^{(k)} P_{T_c}(t - jT_c)$ is a PN randomization sequence which is used to differentiate all the reverse-link users. In (1), P_k is the average transmitted power of the kth user, ω_c is the common carrier frequency, and $\phi^{(k)}$ is the phase angle of the kth modulator to be uniformly distributed in $[0, 2\pi)$. The orthogonal chip duration T_g and the PN chip interval T_c is related to data bit interval T through processing gain $N = T/T_c$. We assume, for simplicity, that T_g is equal to T_c.

2.2. Channel model

From the propagation measurements of the microcellular environments, the multipath Rician fading channel consists of a specular component plus several Rayleigh fading components [14]. The multipath Rician radio channel can be modeled as a modified Rayleigh fading channel by adding a known and constant specular component to the initial tap of the tapped-delay-line representation of the multipath Rayleigh fading channel [15, 16]. Therefore, the complex low-pass impulse response of the multipath Rician fading vector channel associated with kth user may be written as

$$\begin{aligned}\mathbf{h}^{(k)}(\tau) = {} & A^{(k)} \exp\left(j\varphi_0^{(k)}\right) \mathbf{v}\left(\theta_0^{(k)}\right) \delta\left[\tau - \tau_0^{(k)}\right] \\ & + \sum_{l=1}^{L^{(k)}-1} \beta_l^{(k)} \exp\left(j\varphi_l^{(k)}\right) \mathbf{v}\left(\theta_l^{(k)}\right) \delta\left[\tau - \tau_l^{(k)}\right],\end{aligned} \tag{2}$$

with $A^{(k)} = \sqrt{(\alpha^{(k)})^2 + (\beta_0^{(k)})^2}$, where $\alpha^{(k)}$ is the gain of the specular component, and $\beta_l^{(k)}$ refers to the Rayleigh distributed envelope of the lth faded path of the kth user. In (2), $\varphi_l^{(k)}$, $\theta_l^{(k)}$, and $\tau_l^{(k)}$ are phase shift, mean angle of arrival (AOA), and the propagation delay, respectively, of the lth faded path of the kth user. Assuming Rayleigh fading, the probability density function (pdf) of signal strength associated with the kth user's lth propagation path, $l = 0, 1, \ldots, L^{(k)} - 1$, is presented as

$$p\left(\beta_l^{(k)}\right) = \frac{2\beta_l^{(k)}}{\Omega_l^{(k)}} \exp\left(-\frac{(\beta_l^{(k)})^2}{\Omega_l^{(k)}}\right), \tag{3}$$

where $\Omega_l^{(k)}$ is the second moment of $\beta_l^{(k)}$, that is, $E[(\beta_l^{(k)})^2] = \Omega_l^{(k)}$, and we assume it is related to the second moment of the initial path strength $\Omega_0^{(k)}$ for decaying MIP as

$$\Omega_l^{(k)} = \begin{cases} \Omega_0^{(k)} \exp(-l\delta), & \text{for } 0 \le l \le L^{(k)} - 1, \\ & \delta > 0 \text{ (exponential MIP)}, \\ \dfrac{1}{L^{(k)}}, & \text{for } 0 \le l \le L^{(k)} - 1, \\ & \delta = 0 \text{ (uniform MIP)}, \end{cases} \tag{4}$$

where δ reflects the rate at which the decay of average path strength as a function of path delay occurs. In this paper, we consider uniform and exponential delay power profiles. Note that a more realistic profile model may be the exponential MIP [17, 18]. An important parameter that characterizes a Rician fading channel is defined as the ratio of the specular component power to the average power for the initial scattered Rayleigh path, that is, $K_r^{(k)} = (\alpha^{(k)})^2/\Omega_0^{(k)}$, and note that at $K_r^{(k)} = -\infty$ dB, the specular path is absent and the channel is a multipath Rayleigh fading environment [16]. Here, it is assumed that multipath Rician fading channel gain is normalized, that is, $(\alpha^{(k)})^2 + \sum_{l=0}^{L^{(k)}-1}\Omega_l^{(k)} = 1$. The kth user's lth path array response vector is expressed as

$$\mathbf{v}\left(\theta_l^{(k)}\right) = \left[1 \exp\left(\frac{-j2\pi d\cos\theta_l^{(k)}}{\lambda}\right)\cdots\exp\left(\frac{-j2(M-1)\pi d\cos\theta_l^{(k)}}{\lambda}\right)\right]^T, \tag{5}$$

where $\theta_l^{(k)}$ is the mean angle of arrival.

Throughout this paper, we consider that the array geometry, which is the parameter of the antenna aperture gain, is a uniform linear array (ULA) of M identical sensors. All signals from MS arrive at the BS AA with mean AOA $\theta_l^{(k)}$, which are uniformly distributed in $[0, \pi)$.

2.3. Receiver with CS AA

A coherent BPSK modulated RAKE receiver with AA is considered. Perfect power control and perfect channel estimation are assumed, that is, $P_k = P$, $\widehat{A}^{(k)} = A^{(k)}$, and $\widehat{\beta}_l^{(k)} = \beta_l^{(k)}$ for all l and k. The complex received signal is expressed as

$$\begin{aligned}\mathbf{r}(t) = \sqrt{2p}\sum_{k=1}^{K}\Bigg\{&A^{(k)}\mathbf{V}\left(\theta_0^{(k)}\right)b^{(k)}\left(t-\tau_0^{(k)}\right)v^{(k)}\left(t-\tau_0^{(k)}\right)\\ &\times\cos\left[\omega_c t+\psi_0^{(k)}\right]\\ &+\sum_{l=1}^{L^{(k)}-1}\beta_l^{(k)}\mathbf{V}\left(\theta_l^{(k)}\right)b^{(k)}\left(t-\tau_l^{(k)}\right)v^{(k)}\left(t-\tau_l^{(k)}\right)\\ &\times\cos\left[\omega_c t+\psi_l^{(k)}\right]\Bigg\}+\mathbf{n}(t),\end{aligned} \tag{6}$$

where P and $\psi_l^{(k)}$ are the average received power and the phase, respectively, of the lth path associated of the kth user. $\mathbf{n}(t)$ is an $M\times 1$ spatially and temporally white Gaussian noise vector with a zero mean and covariance which is given by $E\{\mathbf{n}(t)\mathbf{n}^H(t)\} = \sigma_n^2\mathbf{I}_M$, where $\mathbf{I}_M$ is the $M\times M$ identity matrix, $\mathbf{n}(t)$ is the Gaussian noise vector, σ_n^2 is the antenna noise variance with $\eta_0/2$, and superscript H denotes the Hermitian transpose operator. When the received signal is matched to the reference user's code, the lth path's matched filter output for the user of interest, $k = 1$, can be expressed as

$$\begin{aligned}\mathbf{y}_l^{(1)} &= \int_{\tau_l^{(1)}}^{\tau_l^{(1)}+T}\mathbf{r}(t)\cdot v^{(1)}\left(t-\tau_l^{(1)}\right)\cos\left[\omega_c t+\psi_l^{(1)}\right]dt\\ &= \mathbf{S}_l^{(1)}+\mathbf{I}_{l,\mathrm{mai}}^{(1)}+\mathbf{I}_{l,\mathrm{si}}^{(1)}+\mathbf{I}_{l,\mathrm{ni}}^{(1)}.\end{aligned} \tag{7}$$

When a training sequence signal is not available, a common criterion for optimizing the weight vector is the maximization of signal to interference-plus-noise ratio (SINR) at the output of the beamformer RAKE. In (7), $\mathbf{u}_l^{(1)} = \mathbf{I}_{l,\mathrm{si}}^{(1)} + \mathbf{I}_{l,\mathrm{mai}}^{(1)} + \mathbf{I}_{l,\mathrm{ni}}^{(1)}$ is a total interference plus noise for the lth path of first user. By solving the following problem, we can obtain the optimal weight to maximize the SINR [19]:

$$\mathbf{w}_{l(\mathrm{opt})}^{(1)} = \max_{\mathbf{w}\neq\mathbf{0}}\frac{\mathbf{w}_l^{(1)^H}\mathbf{R}_{l,yy}\mathbf{w}_l^{(1)}}{\mathbf{w}_l^{(1)^H}\mathbf{R}_{l,uu}\mathbf{w}_l^{(1)}}, \tag{8}$$

where $\mathbf{R}_{l,yy}$and $\mathbf{R}_{l,uu}$ are the second-order correlation matrices of the received signal subspace and the interference-plus-noise subspace, respectively, of first path of first user. Here, $\mathbf{R}_{l,uu}$ can be estimated by the code-filtering approach in [4], which is presented as

$$\mathbf{R}_{l,uu} = \frac{N}{N-1}\left(\mathbf{R}_{rr}-\frac{1}{N}\mathbf{R}_{l,yy}\right), \tag{9}$$

where $\mathbf{R}_{rr}$ means the covariance matrix of the received signal prior to matched filter. The solution is the principal eigenvector corresponded to the largest eigenvalue, $\lambda_{\max}$, of the generalized eigenvalue problem in matrix pair $(\mathbf{R}_{l,yy}, \mathbf{R}_{l,uu})$, which is presented as

$$\mathbf{R}_{l,yy}\cdot\mathbf{w}_{l(\mathrm{opt})}^{(1)} = \lambda_{\max}\cdot\mathbf{R}_{l,uu}\cdot\mathbf{w}_{l(\mathrm{opt})}^{(1)}. \tag{10}$$

From (7) and (8), the corresponding beamformer output for the lth path and user of interest is

$$\begin{aligned}\widehat{z}_l^{(1)} &= \mathbf{w}_l^{(1)^H}\cdot\mathbf{y}_l^{(1)}\\ &= \widehat{S}_l^{(1)}+\widehat{I}_{l,\mathrm{mai}}^{(1)}+\widehat{I}_{l,\mathrm{si}}^{(1)}+\widehat{I}_{l,\mathrm{ni}}^{(1)},\end{aligned} \tag{11}$$

where

$$\hat{S}_l^{(1)} = \sqrt{\frac{P}{2}}\left[\varepsilon \cdot A^{(1)} + (1-\varepsilon)\cdot \beta_l^{(1)}\right] C_{ll}^{(1,1)} b_0^{(1)} T,$$

$$\hat{I}_{l,\mathrm{mai}}^{(1)} = \sqrt{\frac{P}{2}} \sum_{k=2}^{K} \left\{ A^{(k)} C_{l0}^{(1,k)} \left[b_{-1}^{(k)} RW_{k1}\left(\tau_{l0}^{(k)}\right) + b_0^{(k)} \widehat{RW}_{k1}\left(\tau_{l0}^{(k)}\right)\right] \cos\left[\psi_{l0}^{(k)}\right] + \sum_{j=1}^{L^{(k)}-1} \beta_j^{(k)} C_{lj}^{(1,k)} \left[b_{-1}^{(k)} RW_{k1}\left(\tau_{lj}^{(k)}\right) + b_0^{(k)} \widehat{RW}_{k1} \times \left(\tau_{lj}^{(k)}\right)\right] \cos\left[\psi_{lj}^{(k)}\right] \right\},$$

$$\hat{I}_{l,\mathrm{si}}^{(1)} = \sqrt{\frac{P}{2}} \left\{ (1-\varepsilon)\cdot A^{(1)} C_{l0}^{(1,1)} \left[b_{-1}^{(1)} RW_{11}\left(\tau_{l0}^{(1)}\right) + b_0^{(1)} \widehat{RW}_{11}\left(\tau_{l0}^{(1)}\right)\right] \cos\left[\psi_{l0}^{(1)}\right] + \sum_{\substack{j=1 \\ j\neq l}}^{L^{(1)}-1} \beta_j^{(1)} C_{lj}^{(1,1)} \left[b_{-1}^{(1)} RW_{11}\left(\tau_{lj}^{(1)}\right) + b_0^{(1)} \widehat{RW}_{11} \times \left(\tau_{lj}^{(1)}\right)\right] \cos\left[\psi_{lj}^{(1)}\right] \right\},$$

$$\hat{I}_{l,\mathrm{ni}}^{(1)} = \int_{\tau_l^{(1)}}^{\tau_l^{(1)}+T} \mathbf{w}_l^{(1)H} \cdot \mathbf{n}(t) v^{(1)}\left(t-\tau_l^{(1)}\right) \cos\left[\omega_c t + \psi_l^{(1)}\right] dt. \tag{12}$$

Note that $\varepsilon = 1$ for $l = 0$ and $\varepsilon = 0$, otherwise. The parameter $b_0^{(1)}$ being the information bit to be detected, $b_{-1}^{(1)}$ is the preceding bit, $\tau_{lj}^{(k)} = \tau_j^{(k)} - \tau_l^{(1)}$, and $\psi_{lj}^{(k)} = \psi_j^{(k)} - \psi_l^{(1)}$. $\mathbf{w}_l^{(1)} = [w_{l,1}^{(1)} w_{l,2}^{(1)} \cdots w_{l,M}^{(1)}]^T$ is the $M \times 1$ weight vector for the lth path of the first user. $C_{lj}^{(1,k)} = \mathbf{w}_l^{(1)H} \cdot \mathbf{v}(\theta_j^{(k)})$ represents the spatial correlation between the array response vector of the kth user at the jth path and the weight vector for the user of interest at the lth path. RW and $\widehat{RW}$ are continuous partial cross-correlation functions defined by $RW_{k1}(\tau) = \int_0^{\tau} v^{(k)}(t-\tau)\cdot v^{(1)}(t)\,dt$ and $\widehat{RW}_{k1}(\tau) = \int_{\tau}^{T} v^{(k)}(t-\tau)\cdot v^{(1)}(t)\,dt$ [20]. From (11), we can obtain the Rake receiver output from the maximal ratio combining (MRC) $\tilde{z}^{(1)} = A^{(1)}\cdot \hat{z}_0^{(1)} + \sum_{l=1}^{L_r-1} \beta_l^{(1)} \cdot \hat{z}_l^{(1)}$, where the number of fingers L_r is a variable less than or equal to $L^{(k)}$ which is the number of resolvable propagation paths associated with the kth user. In addition, we see that the outputs of the lth branch consist of four terms. The first term represents the desired signal component to be detected. The second term represents the MAI from $(K-1)$ other simultaneous users in the system. The third term is the self-interference (SI) for the user of interest. Finally, the last term is AWGN.

3. PERFORMANCE ANALYSIS OF A CDMA SYSTEM WITH AA IN DISPERSIVE MULTIPATH RICIAN FADING CHANNELS

3.1. Reverse-link asynchronous transmission scenario

To analyze the performance of AA receiver used for the reverse-link asynchronous DS-CDMA system, we employ the Gaussian approximation in the BER calculation, since it is common, and since it was found to be quite accurate even when used for small values of $K(<10)$, provided that the BER is 10^{-3} or higher [21]. Hence, we can treat the MAI and SI as additional independent Gaussian noise and are only interested in their variances. The variance of MAI, conditioned on $\beta_l^{(1)}$, can be expressed as follows:

$$\bar{\sigma}_{\mathrm{mai},l}^2 = \frac{E_b T(N-1)}{6N^2} B^2 \sum_{k=2}^{K} \left[\left(A^{(k)}\zeta_{l0}^{(1,k)}\right)^2 + \sum_{j=1}^{L^{(k)}-1} \Omega_j^{(k)} \left(\zeta_{lj}^{(1,k)}\right)^2 \right], \tag{13}$$

where the channel gain parameter B is $A^{(1)}$ for $l=0$ and $\beta_l^{(1)}$ for $l \geq 1$. The term $E_b = PT$ is the signal energy per bit, and $(\zeta_{lj}^{(1,k)})^2 = E[(C_{lj}^{(1,k)})^2]$ is the second-order characterization of the spatial correlation between the array response vector of the kth user at jth path and the weight vector of user of interest at lth path, of which more detailed derivation is described in the appendix. The conditional variance of $\bar{\sigma}_{\mathrm{si},l}^2$ is approximated by [16, 21]

$$\bar{\sigma}_{\mathrm{si},l}^2 \approx \frac{E_b T}{4N} B^2 \sum_{\substack{j=1 \\ j\neq l}}^{L^{(1)}-1} \Omega_j^{(1)} \left(\zeta_{lj}^{(1,1)}\right)^2. \tag{14}$$

The variance of the AWGN term, conditioned on the value of $\beta_l^{(1)}$, is calculated as

$$\bar{\sigma}_{\mathrm{ni},l}^2 = \frac{T\eta_0 \left(\zeta_{ll}^{(1,1)}\right)^2}{4M} \cdot B^2. \tag{15}$$

Therefore, the output of the receiver is a Gaussian random process with mean

$$U_s = \sqrt{\frac{E_b T}{2}} \left[\left(A^{(1)}\right)^2 \zeta_{00}^{(1,1)} + \sum_{l=1}^{L_r-1} \left(\beta_l^{(1)}\right)^2 \zeta_{ll}^{(1,1)} \right], \tag{16}$$

and the total variance is equal to the sum of the variance of all the interference and noise terms. From (13), (14), and (15), we have

$$\begin{aligned} \bar{\sigma}_T^2 &= \sum_{l=0}^{L_r-1} \left(\bar{\sigma}_{\mathrm{mai},l}^2 + \bar{\sigma}_{\mathrm{si},l}^2 + \bar{\sigma}_{\mathrm{ni},l}^2\right) \\ &= E_b T \left\{ \frac{(N-1)(K-1)[\alpha^2 + \Omega_0 q(L_r,\delta)]\zeta^2}{6N^2} + \frac{\Omega_0 (q(L_r,\delta)-1)\zeta^2}{4N} + \frac{\eta_0 \zeta'^2}{4ME_b} \right\} \left[\alpha^2 + \sum_{l=0}^{L_r-1} \left(\beta_l^{(1)}\right)^2 \right], \end{aligned} \tag{17}$$

where $\Omega_0^{(k)} = \Omega_0$ and $(\alpha^{(k)})^2 = \alpha^2$ for any $k = 1, 2, \ldots, K$. When $\delta > 0$, $q(L_r, \delta) = \sum_{l=0}^{L_r-1} \exp(-l\delta) = 1 - \exp(-L_r\delta)/1 - \exp(-\delta)$, and when $\delta = 0$, $q(L_r, \delta) = L_r$. Note that $(\zeta_{lj}^{(k,m)})^2 = \zeta^2$ when $k \neq m$ or $l \neq j$, and $(\zeta_{lj}^{(k,m)})^2 = \zeta'^2$ when $k = m$ and $l = j$ in the appendix. At the output of the receiver, signal-to-noise ratio (SNR) may be written in a more compact form as γ_s:

$$\gamma_s = \frac{U_s^2}{\tilde{\sigma}_T^2} = \left\{ \frac{(N-1)(K-1)[\alpha^2/\Omega_0 + q(L_r,\delta)]\zeta^2}{3N^2\zeta'^2} + \frac{(q(L_r,\delta)-1)\zeta^2}{2N\zeta'^2} + \frac{\eta_0}{2M\Omega_0 E_b} \right\}^{-1} \cdot \frac{\alpha^2 + \sum_{l=0}^{L_r-1} (\beta_l^{(1)})^2}{\Omega_0}. \tag{18}$$

Assuming the $\beta_l^{(1)}$ are i.i.d. Rayleigh distribution with an exponential MIP, the characteristic function of $X = \sum_{l=0}^{L_r-1} (\beta_l^{(1)})^2$ can be found from [22]:

$$\Psi(j\nu) = \prod_{k=0}^{L_r-1} \frac{1}{1 - j\nu\Omega_k}. \tag{19}$$

Then the inverse Fourier transform of (19) yields the pdf of X:

$$p_X(x) = \sum_{k=0}^{L_r-1} \frac{\pi_k}{\Omega_k} \exp\left(\frac{-x}{\Omega_k}\right). \tag{20}$$

And for the case of a uniform MIP, X has a chi-squared distribution with $2L_r$ degrees of freedom, expressed as

$$p_X(x) = \frac{x^{L_r-1}}{\Omega_0^{L_r}(L_r-1)!} \exp\left(\frac{-x}{\Omega_0}\right). \tag{21}$$

Therefore, the average BER can be found by successive integration given as

$$P_e = \begin{cases} \displaystyle\int_0^\infty Q(\sqrt{\gamma_s}) \cdot \sum_{k=0}^{L_r-1} \frac{\pi_k}{\Omega_k} \exp\left(\frac{-x}{\Omega_k}\right) dx, & \text{for exponential MIP,} \\ \displaystyle\int_0^\infty Q(\sqrt{\gamma_s}) \cdot \frac{x^{L_r-1}}{\Omega_0^{L_r}(L_r-1)!} \exp\left(\frac{-x}{\Omega_0}\right), & \text{for uniform MIP,} \end{cases} \tag{22}$$

where $Q(x) = 1/\sqrt{2\pi} \int_x^\infty \exp(-u^2/2)\, du$ and $\pi_k = \Pi_{i=0, i\neq k}^{L_r-1} x_k/(x_k - x_i) = \Pi_{i=0, i\neq k}^{L_r-1} \Omega_k/(\Omega_k - \Omega_i)$.

3.2. Employment of reverse-link synchronous transmission

In this section, reverse-link synchronous DS-CDMA transmission is considered to make better an estimation of covariance matrices at a beamformer-RAKE receiver. The performance is analyzed to investigate the capacity improvement of the combined AA and RLSTT structure. In RLSTT, the MSs are differentiated by the orthogonal codes and the timing synchronization among mainpaths is achieved with the adaptive timing control in a similar manner to a closed-loop power control algorithm [7]. The arrival time of the initial RAKE receiver branch signal is assumed to be synchronous, while the remaining branch signals are asynchronous, since this can be readily achieved by powerful state-of-art CDMA synchronization techniques [9]. Therefore, here we characterize the scenario, in which the arrival times of the paths are modeled as synchronous for $l = 0$ but as asynchronous in the rest of the branches, that is, $l \geq 1$. Extending (13) by [8] and [13], the variance of the MAI for $l = 0$, conditioned on $\beta_l^{(1)}$, can be expressed as follows:

$$\tilde{\sigma}_{\text{mai},0}^2 = \frac{E_b T(2N-3)}{12N(N-1)} \left(A^{(1)}\right)^2 \sum_{k=2}^{K} \sum_{j=1}^{L^{(k)}-1} \Omega_j^{(k)} \left(\zeta_{0j}^{(1,k)}\right)^2. \tag{23}$$

Similarly, the variance of MAI for $l \geq 1$ is

$$\tilde{\sigma}_{\text{mai},l}^2 = \frac{E_b T(N-1)}{6N^2} \left(\beta_l^{(1)}\right)^2 \times \sum_{k=2}^{K} \left[\left(A^{(k)} \zeta_{l0}^{(1,k)}\right)^2 + \sum_{j=1}^{L^{(k)}-1} \Omega_j^{(k)} \left(\zeta_{lj}^{(1,k)}\right)^2 \right]. \tag{24}$$

From (14), (15), (23), and (24), the SNR at the output of the receiver may be expressed as

$$\gamma_s = \left\{ \frac{(2N-3)(K-1)(q(L_r,\delta)-1)}{6N(N-1)} \times \frac{[\alpha^2 + (\beta_0^{(1)})^2]\zeta_0^2}{\zeta_0'[\alpha^2 + (\beta_0^{(1)})^2] + \zeta' \sum_{l=1}^{L_r-1} (\beta_l^{(1)})^2} + \frac{(N-1)(K-1)[\alpha^2/\Omega_0 + q(L_r,\delta)]}{3N^2} \times \frac{\zeta^2 \sum_{l=1}^{L_r-1} (\beta_l^{(1)})^2}{\zeta_0'[\alpha^2 + (\beta_0^{(1)})^2] + \zeta' \sum_{l=1}^{L_r-1} (\beta_l^{(1)})^2} + \frac{q(L_r,\delta)-1}{2N} \times \frac{\zeta_0^2[\alpha^2 + (\beta_0^{(1)})^2] + \zeta^2 \sum_{l=1}^{L_r-1} (\beta_l^{(1)})^2}{\zeta_0'[\alpha^2 + (\beta_0^{(1)})^2] + \zeta' \sum_{l=1}^{L_r-1} (\beta_l^{(1)})^2} + \frac{\eta_0}{2M\Omega_0 E_b} \times \frac{\zeta_0'^2[\alpha^2 + (\beta_0^{(1)})^2] + \zeta'^2 \sum_{l=1}^{L_r-1} (\beta_l^{(1)})^2}{\zeta'_0[\alpha^2 + (\beta_0^{(1)})^2] + \zeta' \sum_{l=1}^{L_r-1} (\beta_l^{(1)})^2} \right\}^{-1} \times \frac{\zeta'_0[\alpha^2 + (\beta_0^{(1)})^2] + \zeta' \sum_{l=1}^{L_r-1} (\beta_l^{(1)})^2}{\Omega_0}, \tag{25}$$

where $(\zeta_{lj}^{(k,m)})^2 = \zeta_0^2$ when $k \neq m$ or $l \neq j$ for $l = 0$, $(\zeta_{lj}^{(k,m)})^2 = \zeta^2$ when $k \neq m$ or $l \neq j$ for $l > 0$, $(\zeta_{lj}^{(k,m)})^2 = \zeta'^2_0$ when $k = m$ and $l = j$ for $l = 0$, and $(\zeta_{lj}^{(k,m)})^2 = \zeta'^2$ when $k = m$ and $l = j$ for $l > 0$ in the appendix. The average BER performance of reverse-link synchronous DS-CDMA system with AA for the case of a uniform and exponential MIP may

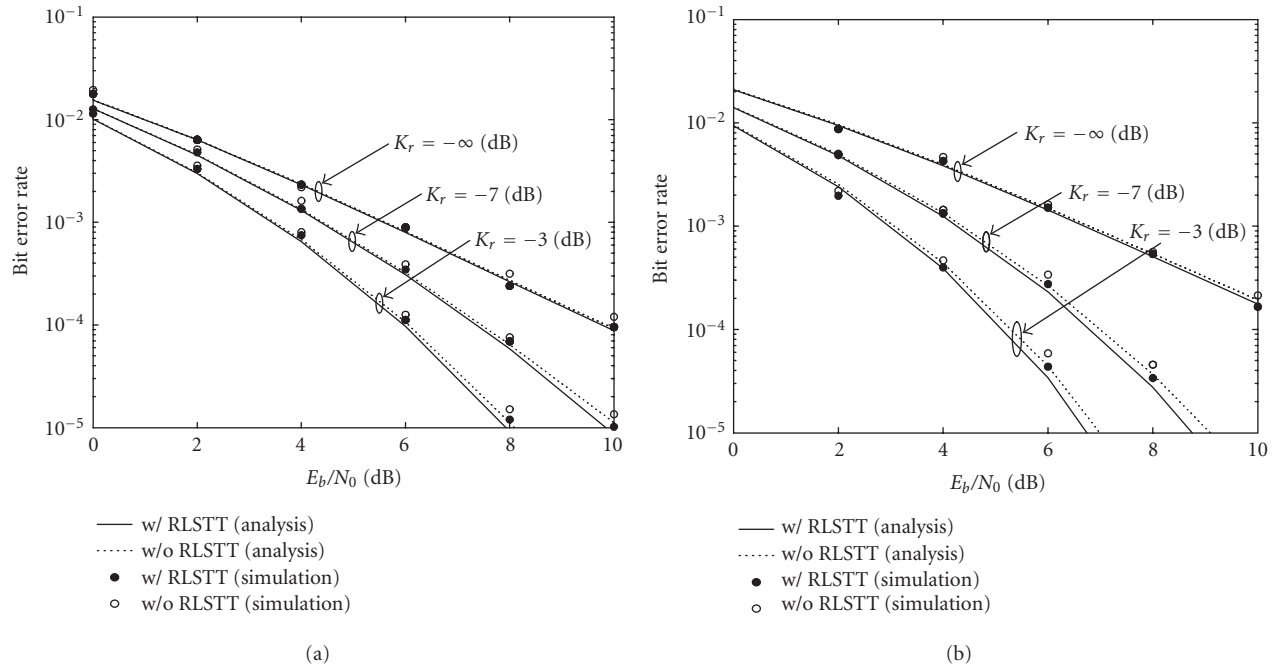

Figure 1: BER versus E_b/N_0 in AA with RLSTT and AA without RLSTT (user = 12, $M = 4$, $L_r = L^{(k)} = 3$, $K_r = -\infty, -7$, and -3 (dB)). (a) $\delta = 0.0$ (uniform MIP). (b) $\delta = 1.0$ (exponential MIP).

be evaluated as

$$P_e = \begin{cases} \displaystyle\int_0^\infty Q(\sqrt{\gamma_s}) \cdot \sum_{k=1}^{L_r-1} \frac{\pi_k'}{\Omega_k} \exp\left(-\frac{x}{\Omega_k}\right) \\ \qquad \cdot \frac{1}{\Omega_0} \exp\left(-\frac{y}{\Omega_0}\right) dxdy, \\ \qquad \text{for exponential MIP}, \\ \displaystyle\int_0^\infty Q(\sqrt{\gamma_s}) \cdot \frac{x^{L_r-2}}{\Omega_0^{L_r-1}(L_r-2)!} \exp\left(-\frac{x}{\Omega_0}\right) \\ \qquad \cdot \frac{1}{\Omega_0} \exp\left(-\frac{y}{\Omega_0}\right) dxdy, \\ \qquad \text{for uniform MIP}, \end{cases} \tag{26}$$

where $\pi_k' = \Pi_{i=1, i\neq k}^{L_r-1} \Omega_k/(\Omega_k - \Omega_i)$. Assuming $X = \sum_{l=1}^{L_r-1} (\beta_l^{(1)})^2$ and $Y = (\beta_0^{(1)})^2$, for exponential MIP, the pdfs of X and Y are $p_X(x) = \sum_{k=1}^{L_r-1} \pi_k'/\Omega_k \exp(-x/\Omega_k)$ and $p_Y(y) = 1/\Omega_0 \exp(-y/\Omega_0)$, for the case of uniform MIP, X and Y have a chi-squared distribution with $2(L_r - 1)$ and 2 degrees of freedom, respectively.

4. NUMERICAL RESULTS

In this paper, we have investigated the BER performance of AA system both with RLSTT and without RLSTT, considering several important factors such as the ratio of the specular component power to the Rayleigh fading power, the shape of MIP, and the number of antennas. In all evaluations, processing gain is assumed to be 128, and the number of paths and taps in RAKE is assumed to be the same for all users and denoted by three, where it includes the specular component. The decaying factor is considered as 1.0 for the exponential MIP and 0.0 for the uniform MIP. The sensor spacing is half the carrier wavelength, and an important parameter that characterizes a Rician fading channel is defined as the ratio of the specular component power to the Rayleigh fading power which is assumed to be the same for all users, that is, $K_r^{(k)} = K_r$.

Figure 1 shows uncoded BER performance as a function of E_b/N_0, when the number of users is twelve, the number of antennas is four, and $K_r = -\infty, -7$, and -3 (dB) are assumed. It is noted that using RLSTT may enhance the achievable performance of the AA system, since RLSTT tends to make better the estimation of covariance matrices for beamformer-RAKE receiver. Furthermore, it is shown that the performance gains between AA with RLSTT and AA without RLSTT increase as the ratio of specular power increases. The results confirm that the analytical results are well matched to the simulation results.

Figure 2 shows the BER system performance as a function of number of antennas, when $E_b/N_0 = 10$ (dB) and the number of users is sixty. The curves are parameterized by different values of $K_r = -3, -2, -1$, and 0 (dB) and indicate that the CS AA system with RLSTT increasingly outperforms the corresponding system without RLSTT when the parameter of K_r increases. Note that comparing Figure 2a and Figure 2b characterizes the effects of increasing the MIP decay factor from $\delta = 0.0$ to $\delta = 1.0$. Intuitively, the received power of the nonfaded specular component increases as the parameter δ increases. This enhances the achievable performance of the system with RLSTT, compared to the system without RLSTT, significantly.

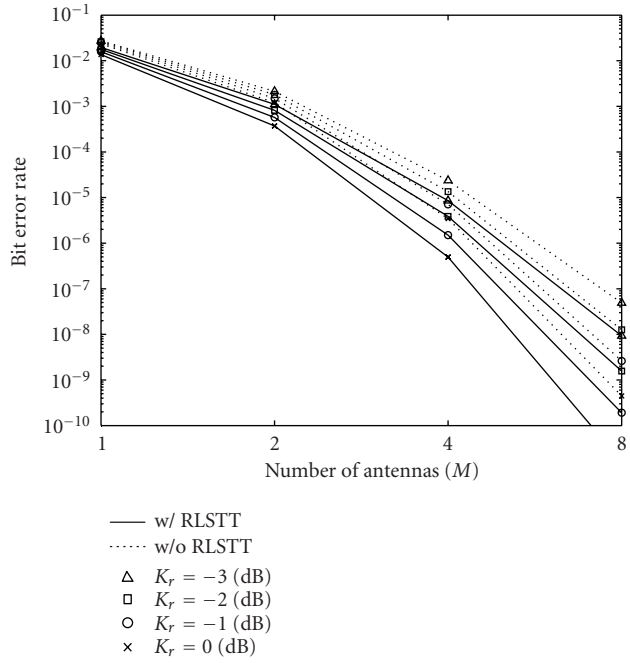

(a)

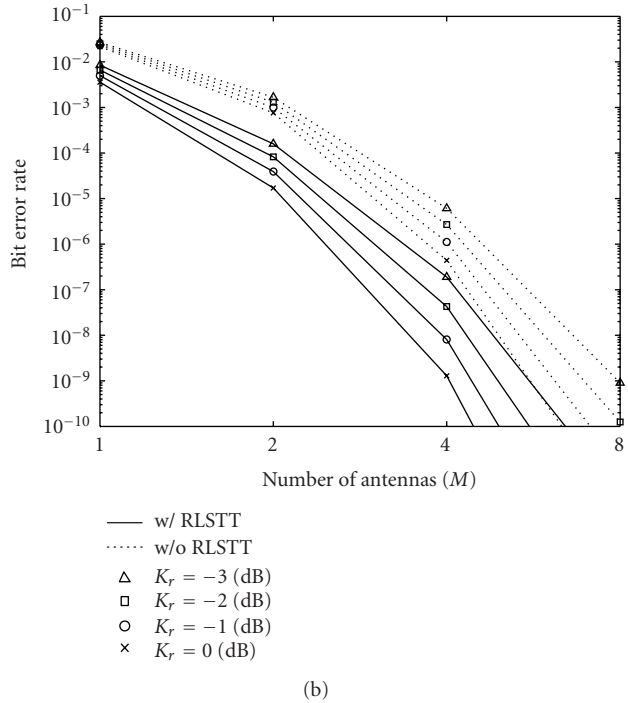

(b)

Figure 2: BER versus number of antennas in AA with RLSTT and AA without RLSTT (user = 60, $E_b/N_0 = 10$ (dB), $L_r = L^{(k)} = 3$, $K_r = -3, -2, -1, 0$ (dB)). (a) $\delta = 0.0$ (uniform MIP). (b) $\delta = 1.0$ (exponential MIP).

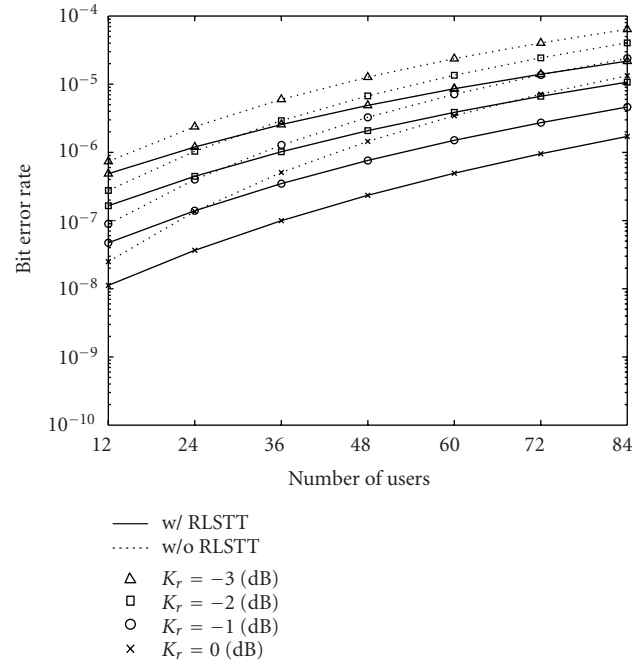

(a)

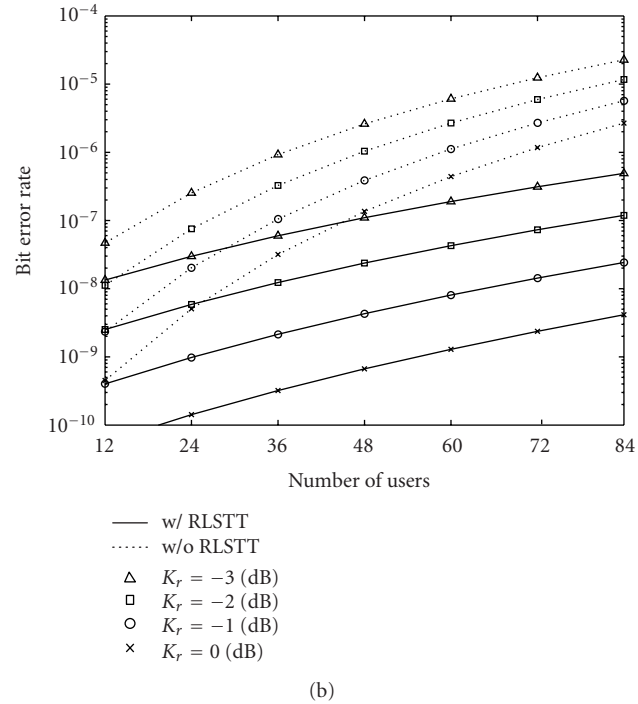

(b)

Figure 3: BER versus number of users in AA with RLSTT and AA without RLSTT ($E_b/N_0 = 10$ (dB), $M = 4$, $L_r = L^{(k)} = 3$, $K_r = -3, -2, -1, 0$ (dB)). (a) $\delta = 0.0$ (uniform MIP). (b) $\delta = 1.0$ (exponential MIP).

In Figure 3, the BER performance is reflected as a function of the number of users, when the various ratios such as $K_r = -3, -2, -1$, and 0 are considered, $E_b/N_0 = 10$ (dB), and the number of antennas is chosen to be four. RLSTT makes a DS-CDMA system with AA insensitive to the number of users and thus increases the achievable overall system capacity. For example, in case of $K_r = 0$ (dB) and $\delta = 0.0$, while AA without RLSTT supports 20 users, AA with RLSTT does more than 35 users at a BER of 10^{-7}, showing the enhancement of 75%. Note that the achievable capacity of the

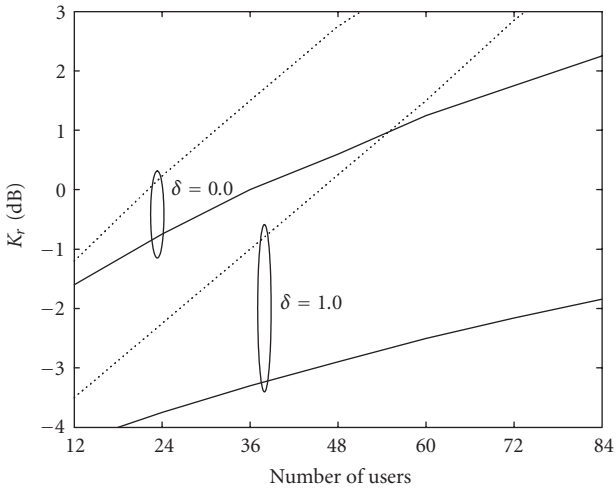

FIGURE 4: Required K_r -factor versus number of users in AA with RLSTT and AA without RLSTT ($E_b/N_0 = 10$ (dB), $M = 4$, $L_r = L^{(k)} = 3$, $\delta = 0.0, 1.0$, BER $= 10^{-7}$).

system with RLSTT, compared to the system without RLSTT, increases as the parameter δ increases.

In Figure 4, the minimum K_r required to achieve BER of 10^{-7} is encounted as a function of the number of users for different decay factors, that is, $\delta = 0.0$ and $\delta = 1.0$, when $E_b/N_0 = 10$ (dB), $M = 4$, and $L_r = L^{(k)} = 3$. The figure demonstrates that while in the exponential MIP of $\delta = 1.0$, AA without RLSTT is required to keep more than 1 (dB) in order to achieve the user capacity of 60 users, AA with RLSTT may make loose the requirement to -3 (dB). The figure can also be used to find the overall system capacity for a given K_r and the decay factor.

5. CONCLUSIONS

In this paper, we presented an improved AA, in which RLSTT is incorporated to effectively make better an estimation of covariance matrices at a beamformer-RAKE receiver. The results show that the addition of an unfaded specular component to the channel model increases the performance difference between with RLSTT and without RLSTT in the CS AA systems. Furthermore, the exponential MIP decay factor has a substantial effect on the system BER performance in a Rician fading channel. These results, however, do not take into account effects such as coding and interleaving. Additionally, it is apparent that RLSTT has superior performance and/or reduces the complexity of the system since AA with RLSTT with fewer numbers of antennas can obtain the better performance than AA without RLSTT.

APPENDIX

SPATIAL CORRELATION STATISTICS

From (10), we can obtain the optimal beamformer weight presented as

$$\mathbf{w}_l^{(k)} = \xi \cdot \left(\mathbf{R}_{l,uu}^{(k)}\right)^{-1} \mathbf{v}(\theta_l^{(k)}), \tag{A.1}$$

since ξ does not affect the SINR, we can set $\xi = 1$. When the total number of paths is large, a large code length yields $\mathbf{R}_{l,uu}^{(k)} = (\sigma_{s,l}^{(k)})^2 \cdot \mathbf{I}_M$ [4]. However, it means that the total undesired signal vector can be modeled as a spatially white Gaussian random vector. Here, $(\sigma_{s,l}^{(k)})^2$ is the total interference-plus-noise power. From (7), the total interference-plus-noise for the lth path of the kth user in the matched filter output is shown as

$$\mathbf{u}_l^{(k)} = \mathbf{I}_{l,\mathrm{si}}^{(k)} + \mathbf{I}_{l,\mathrm{mai}}^{(k)} + \mathbf{I}_{l,\mathrm{ni}}^{(k)}. \tag{A.2}$$

If we assume that the angles of arrival of the multipath components are uniformly distributed over $[0, \pi)$, the total interference vector $\mathbf{I}_{l,si}^{(k)} + \mathbf{I}_{l,\mathrm{mai}}^{(k)}$ will be spatially white [4, Chapter 6]. In this case, the variance of an undesired signal vector is given by

$$\begin{aligned} E\left[\mathbf{u}_l^{(k)} \cdot \mathbf{u}_l{}^{(k)H}\right] &= \left(\sigma_{s,l}^{(k)}\right)^2 \cdot \mathbf{I}_M \\ &= \left[\left(\sigma_{\mathrm{mai},l}^{(k)}\right)^2 + \left(\sigma_{\mathrm{si},l}^{(k)}\right)^2 + \left(\sigma_{\mathrm{ni},l}^{(k)}\right)^2\right] \cdot \mathbf{I}_M, \end{aligned} \tag{A.3}$$

where $(\sigma_{\mathrm{mai},l}^{(k)})^2$ and $(\sigma_{\mathrm{si},l}^{(k)})^2$ are noise variances of MAI and SI in a one-dimension antenna system. In the case of the reverse-link asynchronous DS-CDMA system, we can obtain the variance of the total interference-plus-noise calculated as

$$\left(\sigma_{s,l}^{(k)}\right)^2 = E_b T \left(\frac{(N-1)(K-1)\left[\alpha^2 + \Omega_0 q(L_r, \delta)\right]}{6N^2} + \frac{\Omega_0 (q(L_r, \delta) - 1)}{4N} + \frac{\eta_0}{4E_b} \right) \quad \text{for } l \geq 0. \tag{A.4}$$

For the RLSTT model [7, 16], all active users are synchronous in the mainpath branch. Therefore, the different variances for $l = 0$ and for $l \geq 1$, respectively, are expressed as follows:

$$\begin{aligned} \left(\sigma_{s,0}^{(k)}\right)^2 &= E_b T \left(\frac{(2N-3)(K-1)\Omega_0 (q(L_r, \delta) - 1)}{12N(N-1)} + \frac{\Omega_0 (q(L_r, \delta) - 1)}{4N} + \frac{\eta_0}{4E_b} \right) \quad \text{for } l = 0, \\ \left(\sigma_{s,l}^{(k)}\right)^2 &= E_b T \left(\frac{(N-1)(K-1)\left[\alpha^2 + \Omega_0 q(L_r, \delta)\right]}{6N^2} + \frac{\Omega_0 (q(L_r, \delta) - 1)}{4N} + \frac{\eta_0}{4E_b} \right) \quad \text{for } l \geq 1. \end{aligned} \tag{A.5}$$

Using Hermite polynomial approach we can evaluate the average total interference-plus-noise power per antenna array element. With these assumptions, the optimal beamformer weight of kth user at the lth multipath can be shown to be $\mathbf{w}_l^{(k)} = (\sigma_{s,l}^{(k)})^{-2} \cdot \mathbf{v}(\theta_l^{(k)})$. Therefore, between the array response vector of the mth user at the hth path and the weight vector of the kth user's lth path, the spatial correlation can be

expressed as

$$C_{lh}^{(k,m)} = \frac{\mathbf{v}^H\left(\theta_l^{(k)}\right)\mathbf{v}\left(\theta_h^{(m)}\right)}{\left(\sigma_{s,l}^{(k)}\right)^2} = \frac{CR_{lh}^{(k,m)}}{\left(\sigma_{s,l}^{(k)}\right)^2}, \tag{A.6}$$

where

$$CR_{lh}^{(k,m)} = \sum_{i=0}^{M-1} \exp\left(j\pi \operatorname{si}\cos\theta_l^{(k)}\right)\exp\left(-j\pi \operatorname{si}\cos\theta_h^{(m)}\right),$$
$$s = \frac{2d}{\lambda}. \tag{A.7}$$

The second-order characterization of the spatial correlation is calculated as

$$\left(\zeta_{lh}^{(k,m)}\right)^2 = E\left[\left(C_{lh}^{(k,m)}\right)^2\right] = \frac{E\left[\left(CR_{lh}{}^{(k,m)}\right)^2\right]}{\left(\sigma_{s,l}^{(k)}\right)^4}, \tag{A.8}$$

where

$$\begin{aligned}\left(CR_{lh}^{(k,m)}\right)^2 &= A\left(\theta_l^{(k)}, \theta_h^{(m)}\right)\\ &= \sum_{i=0}^{M-1}(i+1)\exp\left(j\pi \operatorname{si}\cos\theta_l^{(k)}\right)\\ &\quad\times\exp\left(-j\pi \operatorname{si}\cos\theta_h^{(m)}\right)\\ &\quad+\sum_{i=M}^{2(M-1)}(2M-i-1)\exp\left(j\pi \operatorname{si}\cos\theta_l^{(k)}\right)\\ &\quad\times\exp\left(-j\pi \operatorname{si}\cos\theta_h^{(m)}\right).\end{aligned} \tag{A.9}$$

The mean angles of arrival $\theta_l^{(k)}$ and $\theta_h^{(m)}$ have uniform dixstribution in $[0,\pi)$ independently. So,

$$\begin{aligned}&E\left[\left(CR_{lh}^{(k,m)}\right)^2\right]\\ &\quad= \int_0^\pi\int_0^\pi A\left(\theta_l^{(k)}, \theta_h^{(m)}\right)d\theta_l^{(k)}d\theta_h^{(m)}\\ &\quad= \begin{cases}\sum_{i=0}^{M-1}(i+1)J_0(\pi \operatorname{si})J_0(-\pi \operatorname{si})\\ \quad+\sum_{i=M}^{2(M-1)}(2M-i-1)\\ \quad\times J_0(\pi \operatorname{si})J_0(-\pi \operatorname{si}), & k\neq m \text{ or } l\neq h,\\ M^2, & k=m \text{ and } l=h,\end{cases}\end{aligned} \tag{A.10}$$

where $J_0(x)$ is the zero-order Bessel function of the first kind.

REFERENCES

[1] L. C. Godara, "Application of antenna arrays to mobile communications. II. Beam-forming and direction-of-arrival considerations," *Proc. IEEE*, vol. 85, no. 8, pp. 1195–1245, 1997.

[2] A. J. Paulraj and C. B. Papadias, "Space-time processing for wireless communications," *IEEE Signal Processing Mag.*, vol. 14, no. 6, pp. 49–83, 1997.

[3] A. Stephenne and B. Champagne, "Effective multi-path vector channel simulator for antenna array systems," *IEEE Trans. Veh. Technol.*, vol. 49, no. 6, pp. 2370–2381, 2000.

[4] A. F. Naguib, *Adaptive antennas for CDMA wireless networks*, Ph.D dissertation, Stanford University, Stanford, CA, 1996.

[5] J. S. Thompson, P. M. Grant, and B. Mulgrew, "Smart antenna arrays for CDMA systems," *IEEE Pers. Commun.*, vol. 3, no. 5, pp. 16–25, 1996.

[6] W. Ye and A. M. Haimovich, "Performance of cellular CDMA with cell site antenna arrays, rayleigh fading, and power control error," *IEEE Trans. Commun.*, vol. 48, no. 7, pp. 1151–1159, 2000.

[7] E. K. Hong, S. H. Hwang, K. J. Kim, and K. C. Whang, "Synchronous transmission technique for the reverse link in DS-CDMA terrestrial mobile systems," *IEEE Trans. Commun.*, vol. 47, no. 11, pp. 1632–1635, 1999.

[8] S. H. Hwang and D. K. Kim, "Performance of reverse-link synchronous DS-CDMA system on a frequency-selective multipath fading channel with imperfect power control," *EURASIP J. Appl. Signal Process.*, vol. 8, pp. 797–806, 2002.

[9] L. Hanzo, L-L. Yang, E-L. Kuan, and K. Yen, *Single- and Multi-Carrier DS-CDMA*, John Wiley & IEEE Press, 2003.

[10] 3GPP TR25.854, *Uplink Synchronous Transmission Scheme*, May 2001, ftp://ftp.3gpp.org/.

[11] H.-H. Chen, Y.-C. Yeh, C.-H. Tsai, and W.-H. Chang, "Uplink synchronisation control technique and its environment-dependent performance analysis," *IEE Electronics Letters*, vol. 39, no. 24, pp. 1755–1757, 2003.

[12] D. Li, "The perspectives of large area synchronous CDMA technology for the fourth-generation mobile radio," *IEEE Commun. Mag.*, vol. 41, no. 3, pp. 114–118, 2003.

[13] Y. S. Kim, S. H. Hwang, D. K. Cho, and K. C. Whang, *Performance of Antenna Arrays with Reverse-Link Synchronous Transmission Technique for DS-CDMA System in Multipath Fading Channels*, vol. 2402 of *Lecture Notes in Computer Science*, Springer, Heidelberg, 2002.

[14] K. W. Yip and T. S. Ng, "Matched filter bound for multipath Rician-fading channels," *IEEE Trans. Commun.*, vol. 46, no. 4, pp. 441–445, 1998.

[15] J. Wang and L. B. Milstein, "CDMA overlay situations for microcellular mobile communications," *IEEE Trans. Commun.*, vol. 43, no. 234, pp. 603–614, 1995.

[16] S. H. Hwang and L. Hanzo, "Reverse-link performance of synchronous DS-CDMA systems in dispersive rician multipath fading channels," *IEEE Electronics Letters*, vol. 39, no. 23, pp. 1682–1684, 2003.

[17] Rec. ITU-R TG8-1, *Guideline for evaluation of radio transmission technologies for IMT-2000*, 1997, Rec. M.1225.

[18] D. Parsons, *The Mobile Radio Propagation Channels*, Addison-Wesley, 1992.

[19] J. Litva and T. K. Lo, *Digital Beamforming in Wireless Communication*, Artech House, Boston, 1996.

[20] M. Pursley and D. Sarwate, "Evaluation of correlation parameters for periodic sequences," *IEEE Trans. Inform. Theory*, vol. 23, no. 4, pp. 508–513, 1977.

[21] T. Eng and L. B. Milstein, "Coherent DS-CDMA performance in nakagami multipath fading," *IEEE Trans. Commun.*, vol. 43, no. 234, pp. 1134–1143, 1995.

[22] J. G. Proakis, *Digital Communications*, McGraw-Hill, New York, NY, USA, 1983.

Yong-Seok Kim received his B.S. degrees in electronic engineering from the Kyung Hee University, Yongin-si, Korea, in 1998, and M.S. and Ph.D. degrees in communication systems from Yonsei University, Seoul, Korea, in 2000 and 2005, respectively. Since 2005, he has worked for Samsung Electronics. His current research interests include multiantenna system, multiuser communication, and multicarrier system in the 4G communication environments.

Keum-Chan Whang received his B.S. degree in electrical engineering from Yonsei University, Seoul, Korea, in 1967, and the M.S. and Ph.D. degrees from the Polytechnic Institute of New York, in 1975 and 1979, respectively. Since 1980, he has been a Professor in the Department of Electrical and Electronic Engineering, Yonsei University. For the government, he performed various duties such as being a Member of the Radio Wave Application Committee, a Member of Korea Information & Communication Standardization Committee, and is an Advisor for the Ministry of Information and Communication's technology fund and a Director of Accreditation Board for Engineering Education of Korea. Currently, he serves as a Member of Korea Communications Commission, a Project Manager of Qualcomm-Yonsei Research Lab, and a Director of Yonsei's IT Research Center. His research interests include spread-spectrum systems, multiuser communications, and 4G communications techniques.